Journal Name

ARTICLE

A Computational Study of the Phosphoryl Transfer Reaction between ATP and Dha in Aqueous Solution

I. Bordes, J.J. Ruiz-Pernía, R. Castillo* and V. Moliner*

Received 00th January 20xx,
Accepted 00th January 20xx

DOI: 10.1039/x0xx00000x

www.rsc.org/

Phosphoryl transfer reactions are ubiquitous in biology, being involved in processes ranging from energy and signal transduction to the replication genetic material. Dihydroxyacetone phosphate (Dha-P), an intermediate of the synthesis of pyruvate and a very important building block in nature, can be generated converting free dihydroxyacetone (Dha) through the action of Dihydroxyacetone kinase enzyme. In this paper the reference uncatalyzed reaction in solution has been studied in order to define the foundations of the chemical reaction and to determine the most adequate computational method to describe this electronically complex reaction. In particular, the phosphorylation reaction mechanism between adenosine triphosphate (ATP) and Dha in aqueous solution has been studied by means of quantum mechanics/molecular mechanics (QM/MM) Molecular Dynamics (MD) simulations with the QM subset of atoms described with semi-empirical and DFT methods. The results appear to be strongly dependent on the level of calculation, which will have to be taken into account for future studies of the reaction catalyzed by enzymes. In particular, while PM3/MM renders lower free energy barriers and a less endergonic process than AM1d/MM and PM6/MM methods. Nevertheless, the concerted pathway was not located with the former combination of potentials.

Introduction

Phosphoryl transfer, a chemical process that consist on the transfer of the phosphoryl group from a phosphate ester or anhydride to a nucleophile,[1] are involved in a wide range of biological processes, from energy and signal transduction to the replication of genetic material.[2,3] Protein kinases catalyze the transfer of phosphate groups from adenosine triphosphate (ATP) to different substrates. ATP functions as chemical energy carrier[4] since it is a derivative of the nucleic acid adenine that has three high-energy phosphate bonds at the 5' position. It is the most important biological phosphoryl donor required for many enzymatic reactions.[5]

When a phosphate group is transferred from ATP to one of the simplest carbohydrates, for example dihydroxyacetone (Dha), Dha-P is obtained (see Scheme 1).[6] Dha-P is an intermediate for the synthesis of pyruvate[7] and it is a very important C_3 building block in nature since it is used as phosphoryl donor in several enzyme-catalyzed aldol reactions.[8] The phosphorylation of Dha is catalyzed in nature by the action of Dihydroxyacetone kinase enzyme.

Departament de Química Física i Analítica, Universitat Jaume I, 12071 Castellón (Spain)
* to whom correspondence should be addressed:
R. Castillo: rcastill@uji.es
V. Moliner: moliner@uji.es

Electronic Supplementary Information (ESI) available: [PES of the concerted and stepwise mechanisms of the phosphoryl transfer reaction from ATP to Dha in aqueous solution obtained at AM1d/MM (Figure S1), PM3/MM (Figure S2) and PM6/MM (Figure S3). AM1d/MM, PM3/MM solvent assistant mechanism (Figure S4); structures of stationary points of solvent assistant mechanism at AM1d/MM level (Figure S5) and structures of stationary points of solvent assistant mechanism at PM3/MM level (Figure S6). Potential Energies of the mechanisms at AM1d/MM, PM3/MM and PM6/MM (Table 1) and corrected energies at B3LYP (Table S2)]

See DOI: 10.1039/x0xx00000x

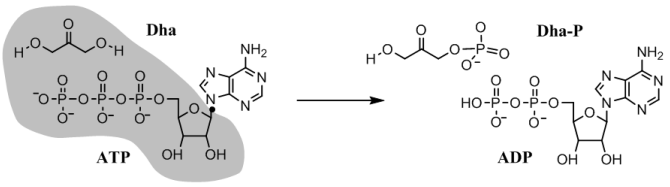

Scheme 1. Schematic reaction between ATP and Dha in aqueous solution, generating ADP and Dha-P. Grey region contains atoms treated quantum mechanically while adenosine group and water molecules (not shown for clarity purposes) are represented by classical force fields. Link atom in ATP is represented as a dot.

The function of kinases has been observed to be deregulated in many human pathological disorders such as cancer. Accordingly, a large number of kinase inhibitors have been developed.[9,10] Nevertheless, despite their multiplicity only part of the kinome has been so far targeted with some specificity and potency, leaving open a broad range of options of future research. Moreover, after decades of research, the molecular mechanisms of phosphoryl transfer reactions remains as a hot topic of debate in the literature,[11] including the controversy of whether the non-enzymatic and the enzymatic reaction proceed by the same molecular mechanism. Remarkably, these reactions present very small non-enzymatic rates and thus require enormous rate accelerations from biological catalysts.[11] The large changes in the charge distribution between reactants and transition state (TS) offers a good advantage for the reaction to be catalyzed[12] and, consequently, a deep knowledge of the reaction in solution becomes even more relevant. Finally, from the computational point of view, a study of the reaction in solution, apart from its interest to quantify the catalytic proficiency of the enzyme, can be used for the calibration and validation of the theoretical approaches to be used in subsequent studies of the corresponding enzyme-catalyzed reaction.[3] In this regard, and as remarked by Kamerlin, an additional difficulty for the theoretical study of the phosphoryl transfer reactions is due to the availability of low-lying d-orbitals on the phosphorus atom which allows the existence of phosphorus pentavalent species as intermediates. Moreover, phosphoryl transfer reactions can potentially occur through multiple equally viable mechanism, even in solution.[2,3]

The phosphoryl transfer from phosphate derivatives to hydroxide ion or to water, namely the hydrolysis reaction, has received a lot of attention in the past years.[2,3,13-16] Regarding the general mechanisms of phosphate derivatives hydrolysis, a debate has been established around whether the reaction proceeds by an associative or dissociative mechanism from the early systematic work of Florian and Warshel.[17] As stated by Warshel and co-workers, some recent computational studies failed to consider the clear distinction between these two paths.[13] Another question of debate is whether the proton from the attacking water molecule is transferred to the terminal phosphate oxygen in a direct way or assisted by additional water molecules.[18] This later possibility was originally explored by Hu and Brinck.[19] More recently, the competition between dissociative/solvent-assisted and associative/substrate-assisted pathways for a number of phosphate and monoesters hydrolysis was examined by Williamd, Kamerlin and co-workers.[20] The authors also considered both direct proton transfer and proton transfer via an intervening leaving group, showing the difference as negligible, and that the substrate-assisted mechanism is only favored with poor leaving groups. Nevertheless, the specific reaction between ATP and Dha has not been studied yet by means of computational methods. The study of this reaction in solution can provide the bedrock for the understanding of the basic chemistry of Dha kinases.

Density functional theory (DFT) and *abinitio* methods have been used in many computational studies of phosphoryl transfer reactions in gas phase or with implicit solvent models.[17,21-23] Nonetheless, the remarkable computation cost of these methods prevents their use to perform MD simulations, which have been shown to be an effective approach to get reaction free energy profiles. An alternative is employing semiempirical methods to treat the QM sub-set of atoms in hybrid QM/MM computational schemes. In the last years, a modified semiempirical Hamiltonian AM1/d-ProT (hereafter simply named as AM1d) has been developed to model phosphoryl transfer reactions.[24] AM1d incorporates d-extension for the phosphorus atom and modified AM1 parameters for oxygen and hydrogen atoms, while the remaining atoms are described at the AM1 level. This semiempirical potential has been shown to provide results in very good agreement with high-level DFT calculations in the study of the hydrolysis of phosphorus compounds.[24-27]

Another semiempirical method that are typically 3-4 orders of magnitude faster than DFT methods, PM3 method[28], has shown to produce a huge stabilization in the energy of phosphorane compounds, resulting from the use of a minimal valence basis.[24] Nevertheless, and despite its accuracy to model phosphoryl transfer reactions is limited because of the lack of *d*orbitals,[16,24] due to its low computational cost, it can be used in order to perform statistical simulations to rapidly explore free-energy surfaces and to establish in a reliable yet computationally feasible way an optimal computational protocol.[16] Several modifications that have been made to the NDDO core-core interaction term have resulted in a more complete parameter optimization called PM6.[29] The most important of these changes were the addition of *d* orbitals to main-group elements and the introduction of diatomic parameters.[30]

A proper comparison between different semiempirical Hamiltonians combined with a common MM force field would allow determining which is the most appropriate one to be used when running long QM/MM MD simulations. Within this target in mind, a theoretical study of the phosphoryl transfer reaction from ATP to Dha in aqueous solution, carried out by means of hybrid QM/MM potentials, is reported in the present paper. Different semiempirical Hamiltonians such as AM1d, PM3 and PM6 have been employed to describe the QM region of the system, while the standard B3LYP hybrid functional has been considered as the reference QM method. As stated above, this study will be the basis for further QM/MM studies of the reaction in the active site of Dha kinases.

Computational methods

Building the system.

The initial coordinates of ATP and Dha were taken from the X-ray structure of *Escherichia coli* dihydroxyacetone kinase, with PDB entry 3PNL.[7] The original ADP molecule was modified to ATP by adding a phosphate group. Then, the two species, ATP and Dha, were solvated with pre-equilibrated cubic box of water molecules of 55.8 Å side. Any water molecules with an oxygen atom lying within 2.8 Å of any non-hydrogen atom of the two solute species were removed. For all simulations, atoms belonging to molecules found at a distance less or equal to 25 Å of one of the phosphorus atom of ATP were defined as flexible. The rest of atoms are kept frozen.

In order to run the simulations with hybrid QM/MM potentials, the sub-set of atoms treated quantum mechanically are those of Dha and part of ATP (phosphate groups and ribose ring, as shown in Scheme 1). When exploring possible mechanisms assisted by solvent, a water molecule was also treated quantum mechanically. To saturate the valence of the QM/MM frontier we used the link atom procedure,[31] placing this atom between C of the ribose molecule and N of the adenine molecule (see Scheme 1). The number of QM atoms is 41, while the system with water molecules contains a total of 17425 atoms.

The part of the ATP not included in the QM region was described by means of the OPLS-AA[32] force field and water molecules with TIP3P force field,[33] as implemented in fDYNAMO library.[34] AM1d/MM and PM3/MM calculations have been carried out with fDYNAMO whereas PM6/MM and B3LYP/MM calculations were performed by combining fDYNAMO with Gaussian09 program.[35] In the case of the DFT/MM calculations, the employed basis set was 6-31G(d,p).

Simulations. First of all, the system was optimized using a combination of steepest descent method and lbfgsb algorithm after relaxation by means of 100 ps of Langevin Dynamics using the NVT ensemble at 300 K with a time step of 1 fs. A switched cutoff, from 14 to 16 Å, was employed for all non-bonded interactions between MM atoms (including the frozen atoms), while the QM region was allowed to interact with every flexible MM atom.

Two phosphorylation reaction paths have been explored without direct participation of water molecules (see Scheme 2); a concerted mechanism and a stepwise mechanism.

The former is the direct transfer of a phosphate group from ATP to Dha, simultaneously with a proton transfer from Dha to the resulting ADP. In the later the transfers are considered in two steps.

Scheme 2. Representation of the two possible reaction mechanisms corresponding to the phosphoryl transfer from ATP to Dha.

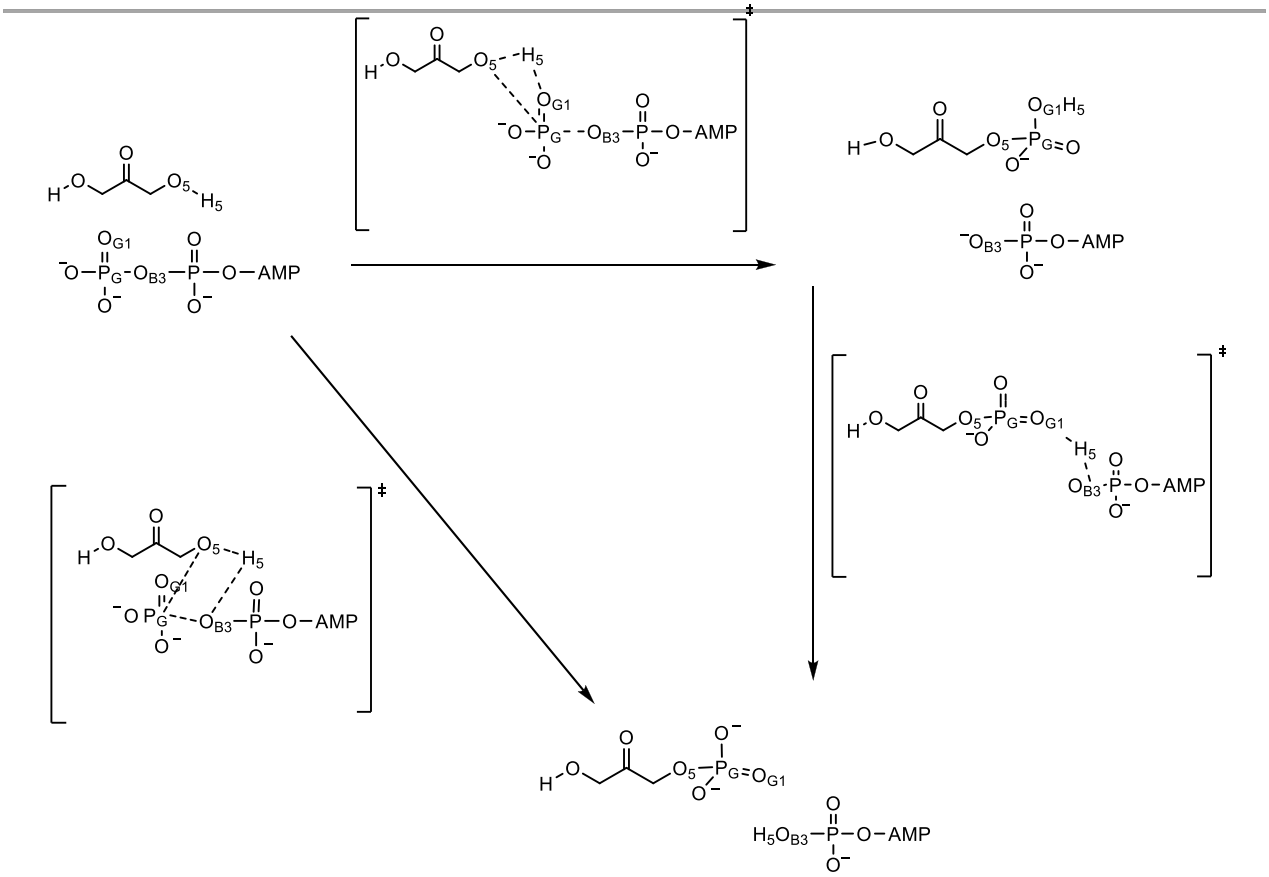

To explore both reaction mechanisms, potential energy surfaces (PESs) were computed by scanning the appropriate combination of the interatomic distances that define both transfers. Later free energy surfaces were computed in terms of potentials of mean force (PMFs).[36] In particular, a two-dimensional QM/MM PMF (2D-PMF) was computed to study the concerted mechanism using, as distinguished reaction coordinates the distance between phosphor PG atom of ATP and the O5 atom of Dha, d(PG-O5), and the antisymmetric combination of the distances describing the hydrogen transfer from Dha to ATP: d(O5-H5)-d(H5-OB3). In the case of the stepwise mechanism, two different PMFs have been explored. In the first one, a 2D-PMF was generated using the distance d(PG-O5) as one of the reaction coordinates and the antisymmetric combination d(O5-H5)-d(H5-OG1) as the other one. The second PMF was traced using the antisymmetric combination d(OG1-H5)-(H5-OB3) as distinguished reaction coordinate, obtaining a 1D-PMF. The umbrella sampling approach[37] was used to constrain the system along the selected values of the reaction coordinates by employing a force constant of 2500 kJ·mol^{-1}·Å^{-2}.

The probability distributions were put together by means of the weighted histogram analysis method (WHAM)[38] to obtain the full probability distribution along the reaction coordinate.

The values of the force constant used for the harmonic umbrella sampling were determined to allow full overlap of the different windows traced in the PMF evaluation, but without losing control over the selected coordinate. Each window consisted of 15 ps of equilibration followed by 20 ps of production. The Verlet algorithm was used to update the velocities. The initial structures in each window of the 2D-PMFs were selected from the corresponding previously generated PESs at the corresponding level of theory, whereas the 1D-PMFs were performed starting from the transition state structure.

Because of the large number of structures that must be evaluated during free energy calculations, QM/MM calculations are usually restricted to the use of semiempirical Hamiltonians.

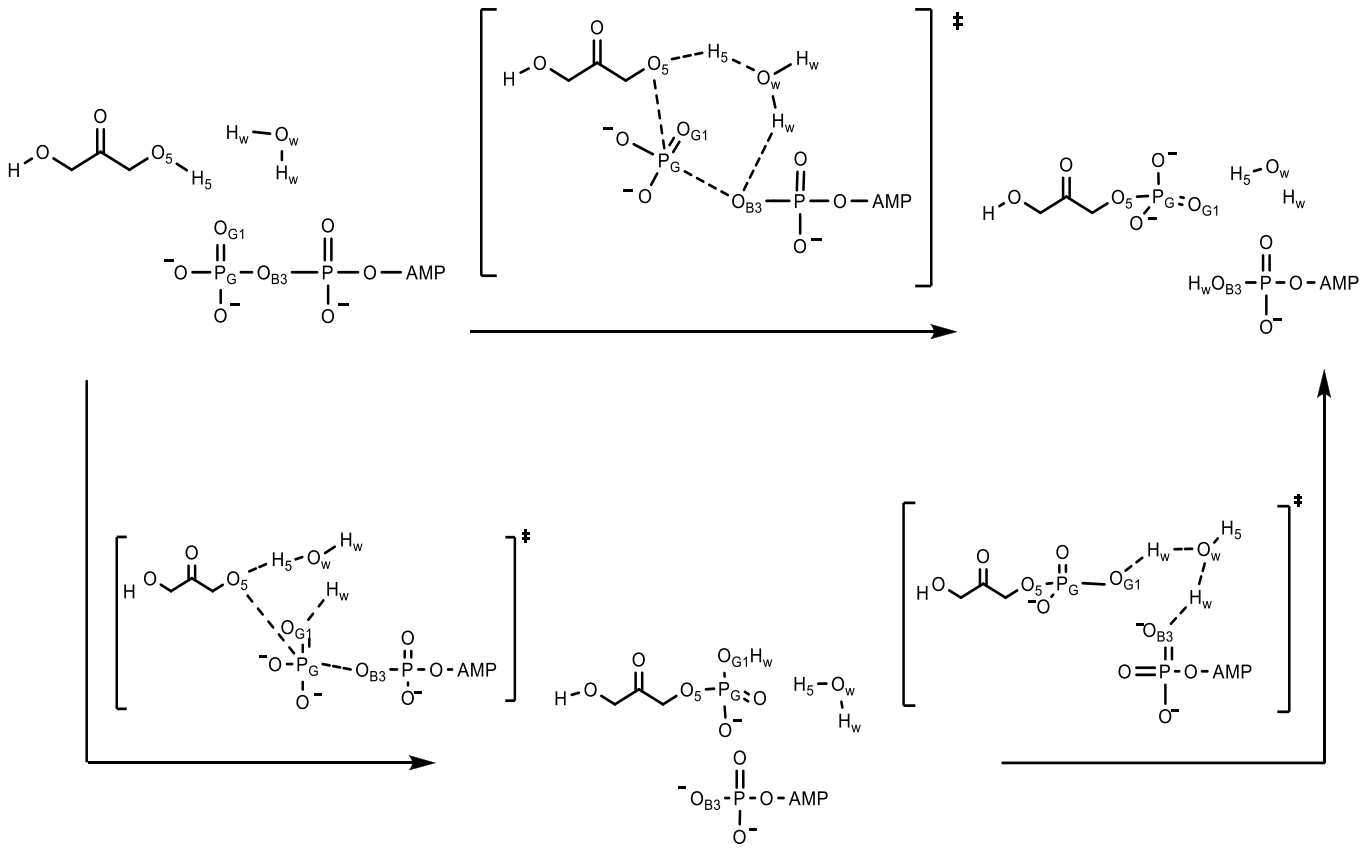

Scheme 3. Representation of the two possible solvent assistant reaction mechanisms corresponding to the phosphoryl transfer from ATP to Dha.

In order to reduce the errors associated with the quantum level of theory employed in our simulations, following the works of Truhlar et al.[39-41] a spline under tension[42,43] is used to interpolate this correction term at any value of the reaction coordinates, ξ_1 and ξ_2 in the case of the 2D-PMFs, or only one coordinate, ξ, for the 1D PMF. Thus, for correction of the 2D-PMFs, we obtain a continuous function in a new energy function to obtain corrected PMFs:[44,45]

$$E = E_{LL/MM} + S[\Delta E_{LL}^{HL}(\xi_1 \xi_2)] \quad (1)$$

where S denotes a two-dimensional spline function, and its argument is a correction term evaluated from the single-point energy difference between a high-level (HL) and a low-level (LL) calculation of the QM subsystem. The selected semiempirical Hamiltonians were used as LL method, while the B3LYP/6-31G(d,p) method was selected for the HL energy calculation. S is adjusted to a defined grid depending on the reaction mechanism studied and the semiempirical Hamiltonian employed. HL single energy calculations are computed on optimized geometries obtained in the corresponding PESs at LL. In the case of the 1D-PMFs, the second step of the stepwise mechanism, the correction scheme is defined as:

$$E = E_{LL/MM} + S[\Delta E_{LL}^{HL}(\xi)] \quad (2)$$

and S is adjusted to a set of points corresponding to the HL single energy calculations on geometries optimized at AM1d and PM3 method, as previously explained. HL calculations were carried out using the Gaussian09 program.

The possible solvent-assisted mechanisms have been explored in terms of PESs since, as demonstrated in next section, the obtained energy barriers were much higher than the ones obtained without participation of explicit water molecules. Then, the much more expensive computing of free energy surfaces was considered as not required to discard these possible paths. Due to the large amount of key coordinates involved in these mechanisms, several anti-symmetrical combinations of distances were tested. The most efficient way to control the process was achieved using, as distinguished reaction coordinates, two antisymmetric combination of distances: the distances describing the hydrogen transfer from Dha to the quantum water molecule, d(O5-H5)-d(H5-Ow), and the antisymmetric combination describing the transfer of phosphate group, d(OB3-PG)-d(PG-O5) (see Scheme 3).

Results and discussion

As stated in previous section, the first step in our study was the exploration of the PESs corresponding to the concerted and stepwise mechanism of the phosphoryl transfer reaction from ATP to Dha in aqueous solution. A QM/MM scheme was used, with the QM region treated by different semiempirical Hamiltonians: AM1d, PM3 and PM6. Then, the resulting PESs (see Figure S1-S3 of Supporting Information) were used to generate the free energy surfaces in terms of 1D- and 2D-PMFs. The results are shown in Figure 1 (AM1d/MM), Figure 2 (PM3/MM) and Figure 3 (PM6/MM), while averaged values of selected interatomic distances of the states located along the reaction paths (reactants, TSs and products states) are listed in Table 1. As observed in Figure S4, the PESs obtained after exploring the solvent-assisted mechanism renders potential energy barriers much higher than the ones obtained without participation of explicit water molecules and, consequently, the 2D PMF were considered as not necessary to be computed for this mechanism (geometries of stationary points located on the PES of this mechanism are reported in Figures S5-S6 of Supporting Information).

Concerted mechanism. Analysis of Figures 1 to 3 reveals that different Hamiltonians can render not only different values of activation and reaction energies, but significant different reaction mechanisms. The first and most dramatic difference when exploring the concerted mechanism is that any attempt to locate a reaction path with PM3/MM method was unsuccessful. On the contrary, the concerted TS obtained by means of AM1d/MM and PM6/MM levels are quite similar, according to the averaged values of the distances PG-O5, PG-OB3, O5-H5 and H5-OB3 listed in Table 1. As observed, both methods describe a TS where the breaking PG-OB3 bond and thePG-O5 forming bond are in a very advanced stage of the reaction, while the H5 transfer would present the opposite behavior being in an earlier stage of the process.

According to the coordination of the phosphorous atom at the TSs, these structures cannot be defined as associative TSs since the PG-OB3 distance in both TSs corresponds to a completely broken bond (3.91 and 3.49 Å in AM1d/MM and PM6/MM, respectively). Interestingly, as observed in Figure 3a, an additional local minimum is located in the reactants valley of the PM6/MM free energy surface that correspond to reactants with a PG-O5 bond significantly shorter (2.42 Å) than in reactants structures obtained at AM1d/MM (3.79 Å) and the absolute minimum of reactants obtained with PM6/MM level (3.11 Å). The corrections of these free energy surfaces at B3LYP/MM level render two different scenarios. Thus, while the AM1d:B3LYP/MM surface can be considered as quite similar to the original AM1d/MM (the quadratic region of the TS appears at values of the two reaction coordinates very close to those obtained in the original AM1/MM surface), the position of the TS at the PM6:B3LYP/MM surface is significantly shifted with respect the original position at the PM6/MM one. Thus, according to the corrected surface, the TS would be described by a H5 atom almost completely transferred (O5-H5 and OB3-H5 distance ca. to 1.62 and 1.07 Å, respectively), while the forming PG-O5 bond would be in a much earlier stage of the reaction (PG-O5 distance ca. 2.3 Å).

From the energetics point of view, the barrier obtained at AM1d/MM level is much higher than the one deduced from the PM6/MM calculations: 35 and 14 kcal·mol^{-1}, respectively. At this point, this huge difference can be related with the relative position of the two species, Dha and ATP, in the reactants. As deduced from the interatomic distances reported in Table 1, PM6/MM reactants state structures are described by the two species significantly closer to each other than reactants state structures located at AM1d/MM

level. This is confirmed by inspection of PG-O5 and OB3-H5 distances which are smaller in the PM6/MM results (3.11 and 2.01 Å, respectively) than in the AM1d/MM results (3.79 and 2.31 Å, respectively). Then, the TS would be closer to reactants state in the PM6/MM free energy surface that in the AM1d/MM and, consequently, a smaller barrier is obtained.

AM1d/MM Concerted mechanism						
distances	**PG-O5**	**PG-OB3**	**PG-PB**	**O5-H5**	**OB3-H5**	**OG1-H5**
R	3.79 ±0.03	1.90 ±0.05	3.37 ±0.07	0.97 ±0.03	2.31 ±0.04	3.43 ±0.61
TS_C	2.02 ±0.03	3.91 ±0.15	4.93 ±0.18	1.07 ±0.03	1.57 ±0.04	3.67 ±0.10
P	1.78 ±0.02	4.33 ±0.33	5.44 ±0.27	3.19 ±0.04	0.97 ±0.03	4.79 ±0.22
AM1d/MM Stepwise mechanism						
R	3.70 ±0.03	1.71 ±0.04	3.01 ±0.07	1.01 ±0.03	3.74 ±0.44	1.86 ±0.04
TS1	2.22 ±0.03	1.75 ±0.05	3.03 ±0.07	2.01 ±0.04	3.33 ±0.08	1.01 ±0.03
I	1.68 ±0.03	3.82 ±0.13	4.46 ±0.24	3.12 ±0.20	1.88 ±0.04	1.03 ±0.03
TS2	1.71 ±0.04	3.52 ±0.12	4.43 ±0.22	3.54 ±0.16	1.18 ±0.03	1.34 ±0.04
P	1.71 ±0.03	3.54 ±0.16	4.95 ±0.18	4.08 ±0.12	1.04 ±0.03	1.76 ±0.04
PM3/MM Stepwise mechanism						
R	3.61 ±0.03	1.77 ±0.04	3.34 ±0.05	0.97 ±0.02	4.12 ±0.15	1.72 ±0.03
TS1-1	3.62 ±0.03	1.74 ±0.04	3.31 ±0.06	1.14 ±0.03	3.53 ±0.13	1.16 ±0.03
I_0	3.73 ±0.03	1.71 ±0.04	3.27 ±0.06	1.71 ±0.03	3.43 ±0.09	0.97 ±0.02
TS1-2	2.44 ±0.03	1.76 ±0.04	3.33 ±0.05	1.77 ±0.03	3.31 ±0.10	0.96 ±0.02
I	1.74 ±0.04	3.86 ±0.11	5.04 ±0.16	3.42 ±0.15	1.77 ±0.03	0.97 ±0.02
TS2	1.77 ±0.04	3.52 ±0.11	4.82 ±0.14	3.60 ±0.16	1.13 ±0.04	1.16 ±0.04
P	1.79 ±0.04	3.75 ±0.20	5.21 ±0.15	3.65 ±0.28	0.97 ±0.02	1.76 ±0.03
PM6/MM Concerted mechanism						
R	3.11 ±0.03	1.74 ±0.05	3.11 ±0.06	1.02 ±0.04	2.01 ±0.05	3.25 ±0.54
R2	2.42 ±0.03	1.76 ±0.05	3.16 ±0.06	1.01 ±0.04	2.05 ±0.05	3.16 ±0.20
TS_C	2.09 ±0.03	3.49 ±0.62	4.69 ±0.63	1.15 ±0.03	1.45 ±0.04	3.62 ±0.17
P	1.76 ±0.03	3.72 ±0.20	4.68 ±0.24	1.75 ±0.04	1.05 ±0.03	4.17 ±0.15
PM6/MM Stepwise mechanism						
R	3.67 ±0.03	1.78 ±0.06	3.13 ±0.07	1.02 ±0.03	4.14 ±0.21	1.77 ±0.04
R2	2.28 ±0.03	1.93 ±0.10	3.24 ±0.09	1.04 ±0.03	4.17 ±0.12	1.86 ±0.04
TS1	2.22 ±0.03	1.77 ±0.05	2.84 ±0.07	1.42 ±0.04	3.58 ±0.08	1.24 ±0.04
I	1.65 ±0.02	6.66 ±0.48	6.99 ±0.85	2.46 ±0.05	8.21 ±0.60	1.03 ±0.04

Table 1. QM/MM averaged key distances (in Å) obtained in the states located along the free energy reaction path of the phosphoryl transfer from ATP to Dha in aqueous solution.

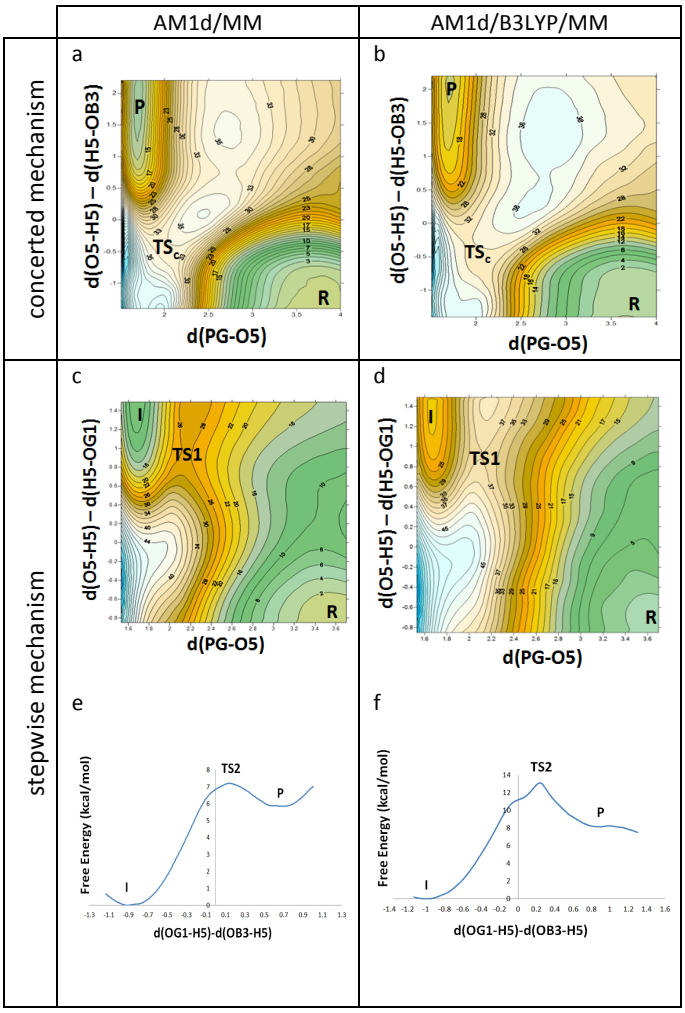

Figure 1. Free energy surfaces of the concerted and stepwise mechanisms of the phosphoryl transfer reaction from ATP to Dha in aqueous solution, obtained as 1D- and 2D- PMFs at AM1d/MM level (panels a, c and e) and with spline corrections at B3LYP/MM level (panels b, d and f). Energies are given in kcal·mol^{-1} and distances in Å.

When the surfaces are corrected at B3LYP/MM level, the resulting free energy barriers are 34 and 55 kcal·mol^{-1} at AM1d:B3LYP/MM and PM6:B3LYP/MM levels, respectively.

As observed, while the original AM1d/MM surface presents a topology quite close to the corrected AM1d:B3LYP/MM one, which is associated to very close free energy barriers (35 and 34 kcal·mol^{-1}, respectively), the fact that corrections of the PM6/MM surface render a dramatic different picture of the topology provoke significantly different barriers (14 and 55 kcal·mol^{-1}, respectively).

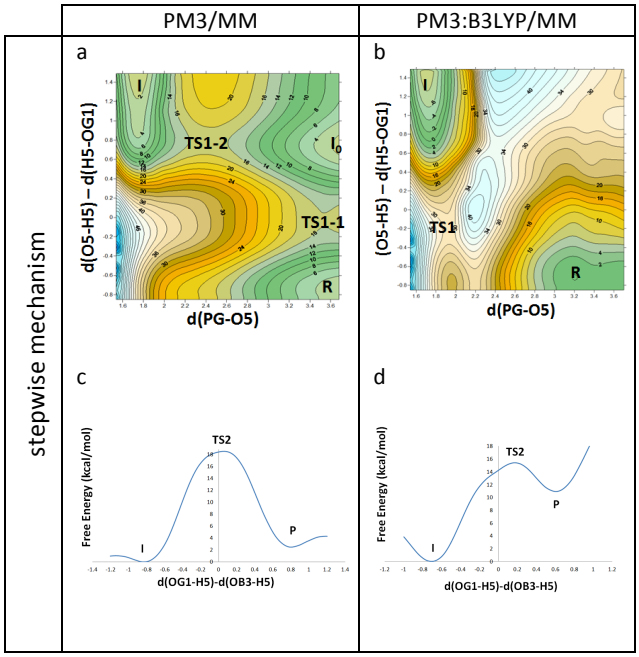

Figure 2. Free energy surfaces of the stepwise mechanism of the phosphoryl transfer reaction from ATP to Dha in aqueous solution, obtained as 1D- and 2D- PMFs at PM3/MM level (panels a and c) and with spline corrections at B3LYP/MM level (panels b and d). Energies are given in kcal·mol^{-1} and distances in Å.

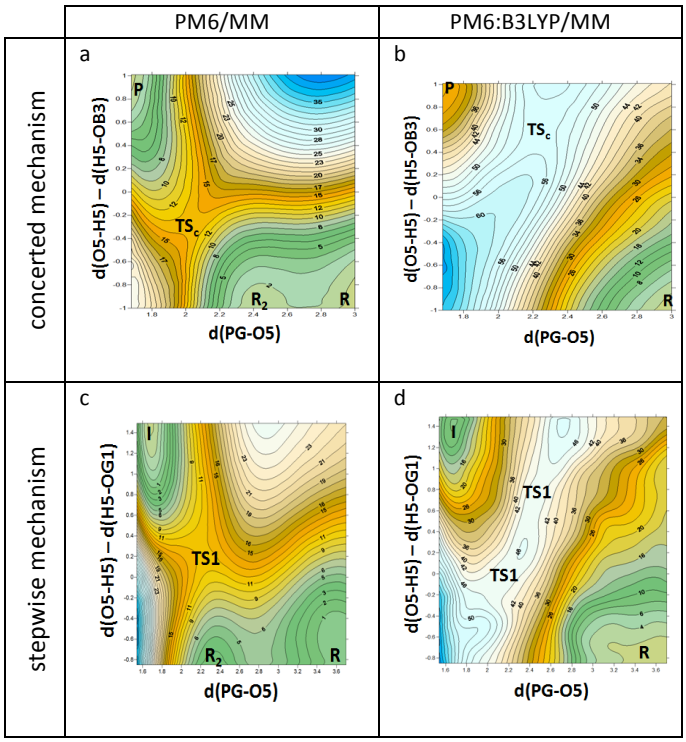

Figure 3. Free energy surfaces of the concerted and stepwise mechanisms of the phosphoryl transfer reaction from ATP to Dha in aqueous solution, obtained as 1D- and 2D- PMFs at PM6/MM level (panels a and c) and with spline corrections at B3LYP/MM level (panels b and d). Energies are given in kcal·mol^{-1} and distances in Å.

Stepwise mechanism. As indicated in Computational Methods section, the first step of this mechanism, from reactants to the intermediate, as depicted in Scheme 2, has been explored through the elaboration of a 2D-PMF and the second step, from the intermediate to products, by a 1D-PMF. The resulting free energy surfaces are shown in Figures 1 to 3. The reaction pathway of the first step obtained by means of AM1d/MM and PM6/MM levels shows a mechanism where the transfer of the phosphate group and the proton transfer occurs simultaneously leading to the intermediate I. However, despite the advance of the phosphate transfer is equivalent in both cases and located in an early stage of the process (distances PG-O5 equal to 2.22±0.03 Å), the location of the TS on both surfaces is clearly different. Thus, while TS1 in the AM1d/MM surface describes an almost completely transferred proton (distances of O5-H5 and OG1-H5 equal to 2.01±0.04 Å and 1.01±0.03 Å, respectively), the PM6/MM method describes a TS1 with the position of the transferred proton almost in between the donor and acceptor atoms (distances of O5-H5 and OG1-H5 equal to 1.42±0.04 Å and 1.24±0.04 Å, respectively). Moreover, a second minimum corresponding to reactants state (R2) is obtained in the PM6/MM free energy surfaces (see Figure 3c), where the two species are in a significant close contact (distance PG-O5 equal to 2.28 ±0.03 Å). This behavior is similar to the one already detected when exploring the concerted mechanism with this PM6/MM method, where a reactant complex closer to the TS was detected (see Figure 3a).

The surface obtained at PM3/MM level is dramatically different to the two surfaces obtained with AM1d/MM and PM6/MM. In this case, an additional minimum corresponding to an intermediate, labeled as I_0 in Figure 2a, is located. According to the averaged values of the interatomic distances, I_0 corresponds to structures where the proton has been transferred to the OG1 atom (distance OG1-H5 equal to 0.97±0.02 Å) while the phosphate is still anchored to the ADP (distance PG-O5 equal to 3.73±0.03 Å). Then, this first step of the PM3/MM stepwise mechanism is, in fact, a stepwise mechanism controlled by TS1-1 and TS1-2, as labeled in Figure 2a.

TS1-1 is associated to the proton transfer and TS1-2 to the phosphate transfer. TS1-2 is similar to the TS1 obtained within the AM1d/MM method, as can be confirmed by analysis of key distances listed in Table 1.

When these free energy surfaces are corrected with spline functions at B3LYP/MM level, interesting observations can be noted. First, the topology of the AM1d:B3LYP/MM surface is almost coincident with the original AM1d/MM, describing a process controlled by TS1 that is basically associated to the phosphate transfer while the proton has been already transferred to the acceptor oxygen atom OG1. On the contrary, the effect of the

corrections on the PM3/MM and PM6/MM free energy surfaces is more dramatic. Thus, the minimum corresponding to the I_0 intermediate located on the PM3/MM disappears after HL corrections and, consequently, the step is a concerted process, as obtained with the other two methods. This step is, nevertheless, described by a quite associative TS1, with a very advanced PG-O5 forming bond, and a proton H5 in an early stage of the transfer to the OG1. Finally, the corrections on the PM6/MM surface render a free energy surface where the second reactant was studied with the AM1d/MM and the PM3/MM methodology, barriers of 7 kcal·mol^{-1} and 18 kcal·mol^{-1}, respectively, where obtained.

Analysis of the key interatomic distances reported in Table 1 reveals an AM1d/MM TS2 with a more advanced proton transfer (H5-OG1 and H5-OB3 distances of TS2 at AM1d/MM level are 1.34±0.04 Å and 1.18±0.03 Å, respectively) than in the PM3/MM TS2 (H5-OG1 and H5-OB3 distances of TS2 at PM3/MM level are 1.16±0.04 Å and 1.13±0.04 Å, respectively).

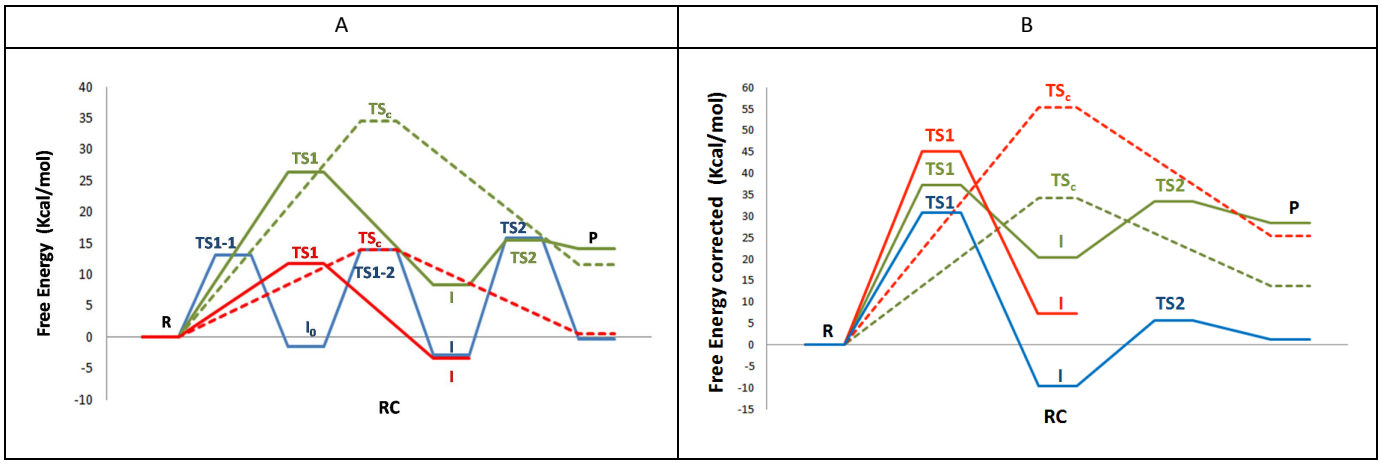

Figure 4. QM/MMfree energy profiles of the two possible reaction mechanisms corresponding to the phosphoryl transfer from ATP to Dha: the stepwise mechanism (solid lines) and the concerted mechanism (dashed lines). **A** panel displays the results from QM/MM calculations with the QM region treated by AM1d (green line), PM3 (blue line) and PM6 (red line). **B** panel displays the results from AM1d:B3LYP/MM (green line), PM3:B3LYP/MM (blue line) and PM6:B3LYP/MM (red line) methods.

minimum (R2 on Figure 3c) has disappeared and the quadratic region of the TS1 appears as a quite extended region. This region covers structures that range from situations where the proton is in between its donor and acceptor atom to TS structures where the proton has been completely transferred to the OG1 atom (see Figure 3d).

From the energetics point of view, the free energy barriers of the first step deduced from the AM1d/MM, PM3/MM and PM6/MM methods are 26, 14 and 12 kcal·mol^{-1}, respectively. After spline corrections at B3LYP/MM level, these barriers are transformed into 37, 31 and 45 kcal·mol^{-1}, respectively. As observed, there is a clear trend in increasing the values, less dramatic in the case of the AM1d/MM method. From the thermodynamic point of view, PM3/MM and PM6/MM describe a first step of the stepwise mechanism as almost thermoneutral while an endergonic reaction is obtained with the AM1d:B3LYP/MM (8 kcal·mol^{-1}).

The free energy surfaces of the second step (from I to P as depicted in Scheme 2) corresponding to the proton transfer from the protonated Dha-P to the ADP to generate the final products, Dha-P and protonated ADP, are shown in Figure 1 and 2 for the AM1d/MM and PM3/MM results, respectively.

First observation that must be noticed is that any effort to transfer the proton from OG1 to OB3 did not render any stable conformation when employing the PM6/MM level. When the step

Moreover, by comparing I with P, more stabilized products are achieved from PM3/MM calculations than from the AM1d/MM calculations (2 kcal·mol^{-1} and 6 kcal·mol^{-1}, respectively). The corrected free energy profiles show a slight increase on the barrier in the case of AM1d:B3LYP/MM (ca. 5 kcal·mol^{-1}) and, in contrast, a slight decrease when using PM3:B3LYP/MM(ca. 3 kcal·mol^{-1}).

The overall free energy profiles for concerted and stepwise mechanisms obtained at the different levels of calculations are compared in Figure 4 while representative snapshots of structures of the located TSs are depicted in Figure 5. The corresponding relative energies to reactants are listed in Table S1 of Supporting Information. As observed in Figure 4, in AM1d/MM method, the stepwise mechanism is favored over the concerted one, but the two mechanisms are very endergonic. The free energy profiles obtained with PM6/MM present lower barriers but with this methodology, it is impossible to localize the final products through the stepwise mechanism. PM3/MM also shows very low free energy barriers, compared with AM1d/MM, to obtain the intermediates and the final product, achieving a high stabilization of both. Keeping in mind the low barriers obtained at PM3/MM level, an alternative possible solvent-assisted mechanism was explored for the rate limiting step of this profile. Nevertheless, the energy barrier was 29 kcal·mol^{-1}, once again much higher than the corresponding step without

participation of a quantum water molecule (see PES in Figure S4 in Supporting Information).

Free energy profiles obtained after B3LYP/MM corrections (see panel B of Figure 4) show how the highest barriers are obtained with the PM6:B3LYP/MM method. Free energy barriers of the stepwise mechanism obtained with AM1d:B3LYP/MM and PM3:B3LYP/MM are quite similar for the first step, but much smaller with the later method.

comparative analysis between different methods, can have implications for further studies of the catalyzed reaction by the action of Dihydroxyacetone kinase.

The first conclusion that can be derived from the calculations is that the possible solvent-assisted mechanisms render significant higher potential energy barriers than the corresponding steps without explicit participation of a water molecule. This possibility was then discarded and attention was focused in exploring the free energy surfaces of the rest of the proposed reaction paths. After exploring the free energy surfaces obtained in terms of 1D and 2D-PMFs for the concerted and stepwise mechanism at AM1d/MM, PM3/MM and PM6/MM level, interesting conclusions can be derived. First of

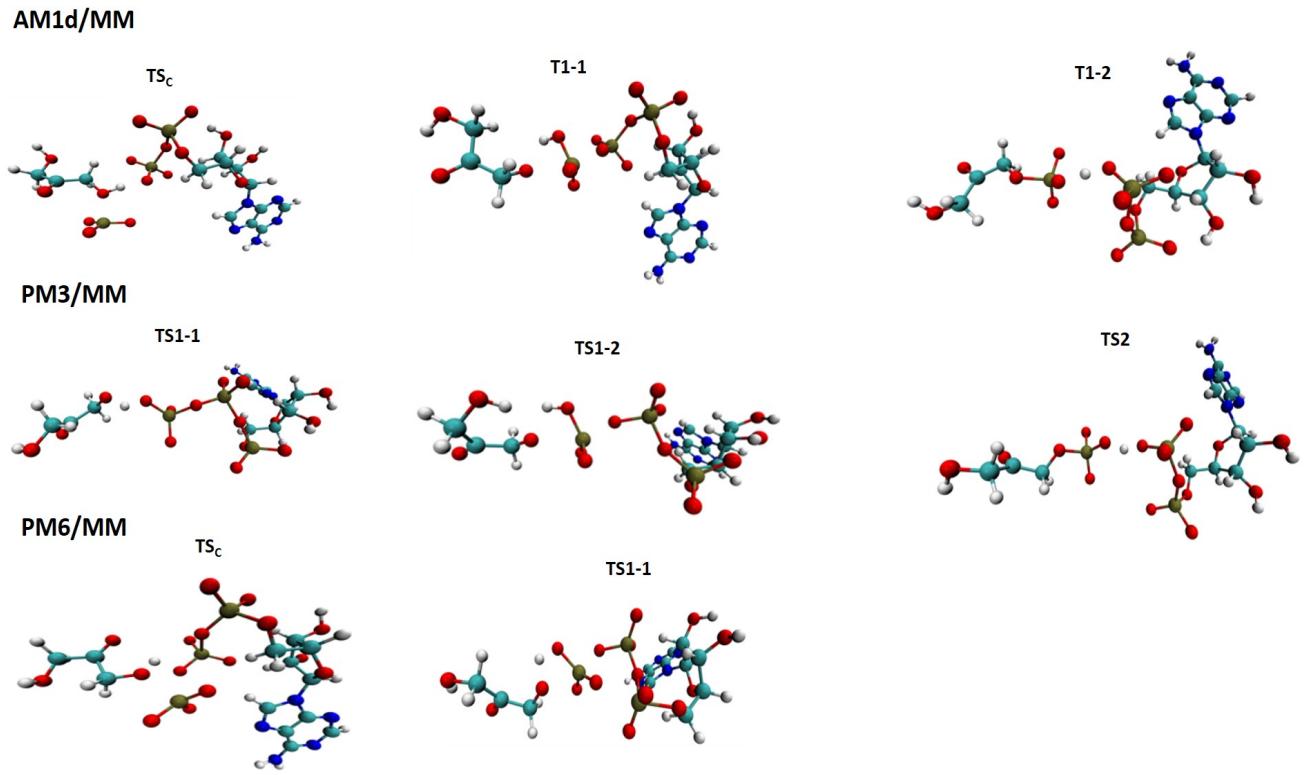

Figure 5. Representative snapshots of structures of the TSs obtained with the different methods. Water molecules are not displayed for clarity purposes. TS_C corresponds to the TS of the concerted mechanism while TS1-1, TS1-2, TS2 corresponds to the different TS along the stepwise mechanism.

Conclusions

In this paper, we have studied the phosphoryl transfer reaction between adenosine triphosphate (ATP) and Dha in aqueous solution within different hybrid QM/MM potentials. In particular, different semiempirical Hamiltonians have been employed to describe the sub-set of atoms treated quantum mechanically, that basically contains the two involved species; ATP and Dha. A deep understanding of the reaction, which is considered as ubiquitous in biology due to the relevance of the formed products, as well as the all, we have demonstrated the high dependency of the results on the selected Hamiltonian. Thus, while AM1d/MM and PM6/MM methods can describe a concerted mechanism, any attempt to obtain this mechanism with PM3/MM was unsuccessful. Regarding the stepwise mechanism, AM1d/MM and PM3/MM were able to describe both steps, phosphate transfer and hydride transfer but, in the case of the PM6/MM method, the second step was not located, being the intermediate (protonated Dha-P) much more stable than the products (protonated ADP). Comparison of the topology of the free energy surfaces of the concerted mechanism obtained with AM1d/MM and PM6/MM methods shows similar location of the quadratic region of the TS, defined by a phosphate transfer in an advanced stage of the process but a proton transfer still bounded to

the Dha moiety. On the contrary, regarding the stepwise mechanism, the location of the TS of the first step obtained with AM1d/MM is quite different to the one obtained with PM6/MM (the phosphate group is transferred after protonation from Dha according to the AM1d/MM method while the opposite timing is obtained with the PM6/MM). PM3/MM renders a surface that describes this step in two-steps; first the transfer of the proton from Dha followed by the protonated phosphate group transfer. This second step is, in fact, similar to the TS1 located with AM1d/MM. The last step of the stepwise mechanism obtained with AM1d/MM and PM3/MM is quite similar regarding the TS, although differences are obtained regarding the thermodynamics of the reaction.

When combining all energetic data of every single step, the full free energy profiles (depicted in Figure 4) show that the stepwise mechanism appears as more favorable than the concerted one when atoms included in the QM region of our QM/MM scheme is described with semiempirical Hamiltonians, being PM3/MM the method rendering the lowest free energy barriers for this stepwise mechanism. This result is reasonable, keeping in mind that the TS of the concerted mechanism requires a non-inline attack (see Figure 5), associated to a higher energy transient conformation. Moreover, the reaction described by the PM3/MM method is almost thermoneutral, while AM1d/MM and PM6/MM methods show endergonic processes. At this point, we must keep in mind that the different products, obtained with the different methods and by exploring the different mechanism, correspond to different product complexes that can differ in the particular conformations and stabilizing inter-molecular interactions. If the reaction was explored up to the completely solvent separated species, the reaction energy should not depend on the mechanism.

Keeping in mind the limitations of the semiempirical methods to describe this kind of reaction that involves phosphor atoms, spline corrections at B3LYP/6-31G(d,p)/MM level have been applied on the previous free energy surfaces. The topology of the resulting high level AM1d:B3LYP/MM free energy surfaces are similar to the previously obtained AM1d/MM ones. The free energy barriers are, nevertheless, slightly raised. On the contrary, high level corrections have significant effects on the PM3/MM surfaces, where the two steps located on the first step of the stepwise mechanism is transformed into a concerted one, and the position of the quadratic region of the TS1 is shifted, becoming closer to the position of the AM1d/MM TS1. The B3LYP/MM correction slightly decreases the free energy barrier. Finally, the effects of the corrections on the PM6/MM surfaces of the concerted mechanism and the first step of the stepwise mechanism are also noticeable. The TS of the concerted mechanism describes a reaction where the proton transfer takes place prior to the phosphate transfer, while the originally TS1 is transformed into a flat and wide quadratic region in the corrected surface.

After this analysis, it appears quite obvious the dependency of the resulting mechanism on the employed method. Moreover, it seems that corrections at B3LYP/MM level render different results depending on the original structures generated during the exploration of the 1D and 2D-PMFs. Thus, in order to look for a convincing proof of the most trustworthy reaction path, PESs have been generated at B3LYP/MM level of theory. We must keep in mind that B3LYP/MM MD calculations are prohibitive from the computational point of view. The resulting surfaces are reported in Figure 6, while structures of the located TSs are displayed in Figure 7.

As observed, and by comparison with the free energy surfaces displayed in Figures 1 to 3, and the corresponding PESs reported in Supporting Information, the results obtained at AM1d/MM are the ones that resemble the most to the B3LYP/MM PESs. This explains the small effect on the topology of the free energy surfaces after B3LYP/MM corrections. Thus, we can confirm the re-parametrized AM1d Hamiltonian as the most convenient semiempirical method to be used in QM/MM MD simulations to explore the reactivity of phosphoryl transfer reactions in terms of free energy surfaces.

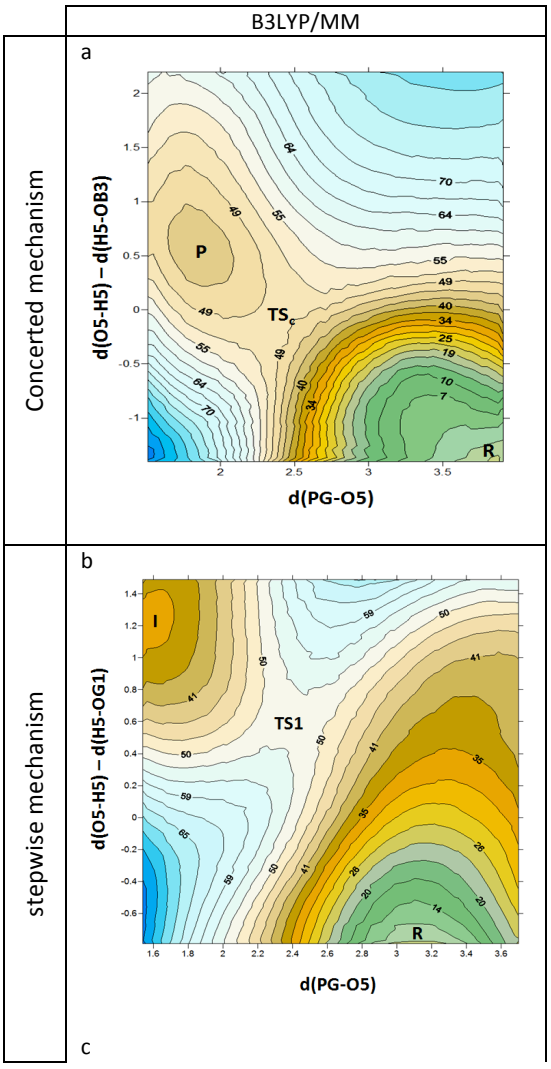

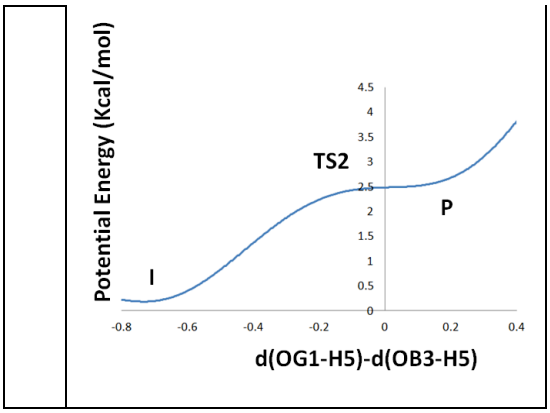

Figure 6. Potential energy surfaces of the concerted (a) and stepwise mechanisms (b and c) of the phosphoryl transfer reaction from ATP to Dha in aqueous solution obtained at B3LYP/MM level. Energies are reported in kcal·mol^{-1} and distances in Å.

The fact that products appear as a shallow minimum in the B3LYP/MM PES of the concerted mechanism (see Figure 6a) could be considered in agreement with the fact that no concerted mechanism was obtained at PM3/MM level. Moreover, as observed on Figure 6c, products complex is less stable than the intermediate in the stepwise mechanism and shows an almost negligible backwards barrier to transform into the intermediate. This could be also considered in agreement with the fact that this second step was not located at PM6/MM level.

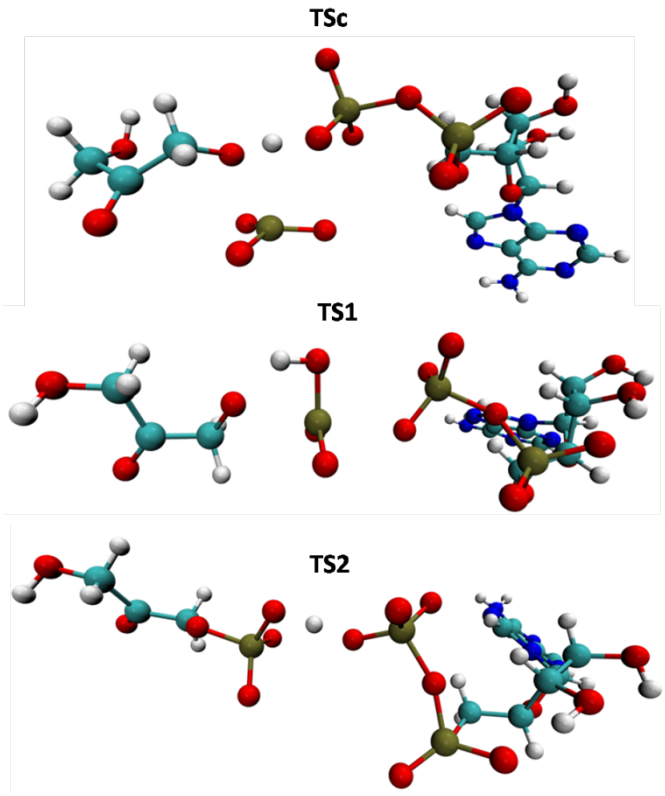

Figure 7. Representative snapshots of structures of the TSs obtained with B3LYP/MM method. Water molecules are not displayed for clarity purposes.

As mentioned, the result of the comparative analysis between different hybrid QM/MM methods applied to the phosphoryl transfer reaction between ATP and Dha in aqueous solution can have implications for further studies of the catalyzed reaction by the action of Dihydroxyacetone kinase. Nevertheless, keeping in mind the features of the reaction, basically, the highly charged involved species, dramatic differences can be expected when including the effect of the protein environment. In particular, positively charged residues and Mg^{2+} ions, that are present in the active site of the kinases, can have an important role in stabilization of transient species. From the technical point of view, these residues should be most probably included in the QM region during the QM/MM because of the presumably large charge reorganization. The analysis of the timescale of protein motions involving these residues will allow having a dynamic description of the process. This prediction is based on previous comparative analysis of chemical reactivity in protein and aqueous environments. Finally, it is important to point out that this study can shed some light in the debate about the kind of TSs governing similar reactions involving phosphate groups.

Acknowledgments

This work was supported by the Spanish Ministerio de Economia y Competitividad (project CTQ2012-36253-C03-01), Generalitat Valenciana (project Prometeo II/2014/022) and Universitat Jaume I (project P1·1B2013-58). The authors acknowledge computational facilities of the Servei d'Informàtica of Universitat Jaume I.

Notes and references

1 A. C. Hengge, In Phosphoryl Transfer Reactions, Eds.; John Wiley & Sons, 2001.
2 S. C. L. Kamerlin, N. H. Williams, A. Warshel, *Journal of Organic Chemistry,* 2008, **73**, 6960.
3 S. C. L. Kamerlin, *Journal of Organic Chemistry,* 2011, **76**, 9228.
4 C. Bachler, K. Flukiger-Bruhwiler, P. Schneider, P. Bahler, B. Erni, *Journal of Biological Chemistry*, 2005, **280**, 18321.
5 S. Iwamoto, K. Motomura, Y. Shinoda, M. Urata, J. Kato, N. Takiguchi, H. Ohtake, R. Hirota, A. Kuroda, *Applied and Environmental Microbiology*, 2007, **73**, 5676.
6 B. Erni, C. Siebold, S. Christen, A. Srinivas, A. Oberholzer, U. Baumann, *Cellular and Molecular Life Sciences*, 2006, **63**, 890.
7 R. Shi, L. McDonald, Q. Cui, A. Matte, M. Cygler, I. Ekiel. *Proceedings of the National Academic of Sciences of the United States of America*, **108**, 1302.
8 D. Enders, M. Voith, A. Lenzen, *Angewandte Chemie International Edition*, 2005, **44**, 1304.
9 J. Colinge, A. Cesar-Razquin, K. Huber, F. P. Breitwieser, P. Majek, G. Superti-Furga, *Journal of Proteomics,* 2014, **107**, 113.
10 H. Weinmann, R. Metternich, *ChemBioChem,* 2005, **6**, 455.

11 J. K. Lassila, J. G. Zalatan, D. Herschlag, *In Annual Review of Biochemistry*, R. D. Kornberg, C. R. H. Raetz, J. E. Rothman, J. W. Thorner, 2011, Vol. **80**, 669.

12 R. P. Bora, M. J. L. Mills, M. P. Frushicheva, A. Warshel, *Journal of Physical Chemistry B,* 2015, **119**, 3434.

13 B. L. Grigorenko, A. V. Rogov, A. V. Nemukhin, *Journal of Physical Chemistry B,* 2006, **110**, 4407.

14 C. B. Harrison, K. Schulten, *Journal of Chemical Theory and Computation,* 2012, **8**, 2328.

15 F. Xia, K. Tian, H. Zhu, *Journal of Chemical Theory and Computation,* 2013, **1017**, 60.

16 N. V. Plotnikov, B. R. Prasad, S. Chakrabarty, Z. T. Chu, A. Warshel, *Journal of Physical Chemistry B,* 2013, **117**, 12807.

17 J. Florian, A. Warshel, *Journal of Physical Chemistry B,* 1998, **102**, 719.

18 S. C. Kamerlin, P. K. Sharma, R. B. Prasad, A. Warshel, *Quarterly Reviews of Biophysics,* 2013, **46**, 1.

19 C. H. Hu, T. Brinck, *Journal of Physical Chemistry A,* 1999, **103**, 5379.

20 F. Duarte, J.Aqvist, N. H. Williams, S. C. L. Kamerlin, *Journal of the American Chemical Society*, 2015, **137**, 1081-1093.

21 Y. Liu, X. Lopez, D. M. York, *Chemical Communications,* 2005, 3909.

22 X. Lopez, A. Dejaegere, F. Leclerc, D. M. York, M. Karplus, *Journal of Physical Chemistry B,* 2006, **110**, 11525.

23D. G. Xu, H. Guo, Y. Liu, D. M. York, *Journal of Physical Chemistry B,* 2005, **109**, 13827.

24 K. Nam, Q. Cui, J. Gao, D. M. York, *Journal of Chemical Theory and Computation,* 2007, **3**, 486.

25 V. Lopez-Canut, S. Marti, J. Bertran, V. Moliner, I. Tuñón, *Journal of Physical Chemistry B,* 2009, **113**, 7816.

26 V. Lopez-Canut, J. Javier Ruiz-Pernia, R. Castillo, V. Moliner, I. Tuñón, *Chemistry-A European Journal,* **2012**, *18*, 9612.

27 V. Lopez-Canut, M. Roca, J. Bertran, V. Moliner, I. Tuñón, *Journal of the American Chemical Society,* 2011, **133**, 12050.

28 J. J. P. Stewart, *Journal of Computational Chemistry,* 1989, **10**, 209.

29 Y. Zhao, D. G. Truhlar, *Theoretical Chemistry Accounts,* 2008, **120**, 215.

30 J. J. P. Stewart, *Journal of Molecular Modeling,* 2007, **13**, 1173.

31 M. J. Field, P. A. Bash, M. Karplus, *Journal of Computational Chemistry,* 1990, **11**, 700.

32 W. L. Jorgensen, J. Tiradorives, *Journal of the American Chemical Society,* 1988, **110**, 1657.

33 W. L. Jorgensen, J. Chandrasekhar, J. D. Madura, R. W. Impey, M. L. Klein, *Journal of Chemical Physics,* 1983, **79**, 926.

34 M. J. Field, M. Albe, C. Bret, F. Proust-De Martin, A. Thomas, *Journal of Computational Chemistry,* 2000, **21**, 1088.

35 M. J. Frisch, G. W. Trucks, H. B. Schlegel, G. E. Scuseria, M. A. Robb, J. R. Cheeseman, G. Scalmani, V. Barone, B. Mennucci, G. A. Petersson, H. Nakatsuji, M. Cariaco, X. Li, H. P. Hratchian, A. F. Izmaylov, J. Bloino, G. Zheng, J. L. Sonnenberg, M. Hada, M. Ehara, K. Toyota, R. Fukuda, J. Hasegawa, M. Ishida, T. Nakajima, Y. Honda, O. Kitao, H. Nakai, T. Vreven, J. A. Montgomery, Jr., J. E. Peralta, F. Ogliaro, M. Bearpark, J. J. Heyd, E. Brothers, K. N. Kudin, V. N. Staroverov, R. Kobayashi, J. Normand, K. Raghavachari, A. Rendell, J. C. Burant, S. S. Iyengar, J. Tomasi, M. Cossi, N. Rega, J. M. Millam, M. Klene, J. E. Knox, J. B. Cross, V. Bakken, C. Adamo, J. Jaramillo, R. Gomperts, R. E. Stratmann, O. Yazyev, A. J. Austin, R. Cammi, C. Pomelli, J. W. Ochterski, R. L. Martin, K. Morokuma, V. G. Zakrzewski, G. A. Voth, P. Salvador, J. J. Dannenberg, S. Dapprich, A. D. Daniels, O. Farkas, J. B. Foresman, J. V. Ortiz, J. Cioslowski, D. J. Fox; Gaussian 09, Revision A. 2. Wallingford CT: Gaussian; Inc, **2009**.

36 B. Roux, *Computer Physics Communications,* 1995, **91**, 275.

37 G. M. Torrie, J. P. Valleau, *Journal of Computational Physiscs,* 1977, **23**, 187.

38 S. Kumar, D. Bouzida, R. H. Swendsen, P. A. Kollman, J. M. Rosenberg, *Journal of Computational Chemistry,* 1992, **13**, 1011.

39 J. C. Corchado, E. L. Coitino, Y. Y. Chuang, P. L. Fast, D. G. Truhlar, *Journal of Physical Chemistry A,* 1998, **102**, 2424.

40 K. A. Nguyen, I. Rossi,D. G. Truhlar, *Journal of Chemical Physics,*1995, **103**, 5522.

41 Y. Y. Chuang, J. C. Corchado, D. G. Truhlar, *Journal of Physical Chemistry A,* 1999, **103**, 1140.

42 R. J. Renka, *Siam Journal of Scientific and Statistical Computing,* 1987, **8**, 393.

43 R. J. Renka, *Acm Transactions on Mathematical Software,* 1993, **19**, 81.

44 J. J. Ruiz-Pernia, E. Silla, I. Tuñon, S. Marti, *Journal of Physical Chemistry B,* 2006, **110**, 17663.

45 S. Ferrer, S. Marti,V. Moliner, I. Tuñón, J. Bertran, *Physical Chemistry Chemistry Physics,*2012, **14**, 3482.

